

# VOLUME EFFECT ON CLEAVAGE STRENGTH, MICROSTRUCTURE AND FRACTURE MICROMECHANISM OF WELDED 15MnVN STEEL

Hou Chun-xiao\*, Cai Qi-gong\*\*, Su Yi\* and Zheng Xiu-yuan\*\*\*

*\*Department of Mechanical Engineering, Qinghua University, Beijing, China*

*\*\*Iron and Steel Research Institute, Beijing, China*

*\*\*\*Department of Engineering Mechanics, Qinghua University, Beijing, China*

## ABSTRACT

Tests on cleavage fracture of smooth, notched and cracked specimens of simulated HAZ structure for 15MnVN steel show that the measured cleavage strength,  $\sigma_f^*$ , defined by the maximum principal stress at fracture varies with the volume involved in fracture process. Metallographic and SEM examination of fracture specimens lead to the conclusion that the cleavage fracture of the welded structure initiates at the crack nuclei formed in granular islands of M-A constituents and propagates into the ferrite matrix. In order to clarify the volume effect on cleavage stress for different specimen geometries, Weibull type statistical formulae are derived based on the 'weakest link theory' and the measured size distribution of M-A constituents. The volume effect on measured cleavage stresses of smooth, notched and cracked specimens are then explained.

## KEYWORDS

Volume effect; cleavage strength; simulated HAZ structure; fracture micro-mechanism; Weibull type statistical formula.

## INTRODUCTION

It has been assumed that cleavage fracture follows a critical tensile stress criterion (Knott, 1966). Ritchie, Knott and Rice (1973) further pointed out that for a cracked specimen the stress in front of the crack tip has to exceed the cleavage stress over a characteristic distance  $X_0$  in order to promote an unstable fracture. Thus, definition and correct measurement of the cleavage stress,  $\sigma_f^*$ , is a rather important task.

$\sigma_f^*$  is usually measured by using single-edge notch bend (SENB) specimen (of 12.7 mm square cross-section) under 4-point pure bending (Ritchie, Knott and Rice, 1973; Curry and Knott, 1976). It is defined as the maximum principal stress within notch-root region at cleavage fracture initiation. However, by using notched tensile specimens with different notch-root radii in cleavage fracture testing, Beremin (1981) has come to the conclusion that the value

of the measured cleavage stress is dependent on the volume involved in the fracture process, but no quantitative relationship has been given.

The aim of the present work is to clarify the relationship between the cleavage fracture stress and the volume involved in the brittle fracture process. Smooth, notched and cracked specimens were used in testing. The cleavage fracture stress in cracked specimens is defined as the maximum principal stress within the crack tip region at cleavage fracture initiation. Metallographic and SEM examinations were performed on the fractured specimens in order to assess the micromechanism of cleavage fracture of the simulated heat-affected zone (HAZ) structure for welded 15MnVN steel. Statistical and fracture-mechanical analyses of the cleavage fracture are conducted to derive the Weibull type formulae for the cleavage fracture for smooth, notched and cracked specimens. Finally, the volume effect on cleavage stress defined and measured for different kinds of specimens is interpreted by using these formulae. The relationship between the cleavage stress,  $\bar{\sigma}_f^*$ , and the effective volume,  $V_e$ , involved in fracture process is derived and compared with the experiment.

#### EXPERIMENTATION

The chemical composition of 15MnVN steel used in this experiment is listed in table 1.

Table 1. Chemical composition of the steel used

Composition	C	Si	Mn	V	N	P	S
Wt. %	0.195	0.44	0.172	0.152	0.016	0.016	0.025

In order to obtain a similar micro-structure and grain size in overheated zone of HAZ of the welded 15MnVN steel with 30KJ/cm heat input under submerged arc automatic welding condition, a resistance heating thermosimulating machine was used. The specimens were treated by the following simulated thermo-cycle: highest temperature of 1250°C, retention time of 9sec above 1100°C, and the cooling time of 77sec from 800°C to 500°C. The specimens were then notched and precracked at the region with thermo-simulated structure as shown in Fig. 1.



Fig. 1. Specimen geometry (in mm), the shaded area denotes thermo-simulated structure.

$J_{1c}$  values were measured from -102°C to room temperature and were converted to  $K_{1c}$  values. Yield strength,  $\bar{\sigma}_{0.2}$ , and strain hardening exponent,  $n$ , from -196°C to room temperature were measured by compressing specimens cut from simulated HAZ with 12 mm height and 8 mm in diameter.

Cleavage stresses,  $\bar{\sigma}_f^*$ , for notched specimens were determined by 4-point bending at -100°C, for smooth specimens by tension test at -196°C using tensile specimens of 10 mm gauge length and 3 mm in diameter.

The microstructure, crack initiation site and crack propagation mode were examined by optical and scanning electron microscopes. The thickness-size distribution of M-A constituents which serves as the crack nuclei was also obtained.

#### EXPERIMENTAL RESULTS

Regression analysis of the measured  $\bar{\sigma}_{0.2}$  from -196°C to 18°C shows that the yield strength of the simulated structure at various temperatures can be expressed by the following regression formula

$$\bar{\sigma}_{0.2} = 3201.25 (273 + T)^{-0.274} \quad (\text{MPa})$$

The mean values of cleavage stresses,  $\bar{\sigma}_f^*$ , measured by 4-point bending of notch specimens and by tension test of smooth specimens are listed in Table 2.

Table 2. Experimental and computed results

Kind of specimen	Specimen number	T°C	$K_{1c}$ MPam	$\bar{\sigma}_f^*$ MPa	$V_e$ mm <sup>3</sup>
Smooth specimen	3	-196		1432.1	119.37
Notched specimen	4	-100		1994.1	2.863
Cracked specimen	7	-80	50.19	3088.6	$17.66 \times 10^{-3}$
Cracked specimen	7	-102	45.03	3259.1	$9.25 \times 10^{-3}$

The mean values of  $K_{1c}$  and  $\bar{\sigma}_f^*$  of tested cracked specimens are also listed in it. The cleavage stress,  $\bar{\sigma}_f^*$ , of a cracked specimen is defined by  $\bar{\sigma}_f^* = R \cdot \bar{\sigma}_{0.2}$ , where the stress intensification factor R is given by McMeeking (1977).

#### CLEAVAGE INITIATION SITE

The microstructure of simulated HAZ of 15MnVN steel consists of proeutectoid ferrite network along prior austenitic grain boundaries, acicular ferrite and M-A constituents. The small islands in Fig. 2 are M-A constituents. The high carbon martensite in M-A constituent is hard and brittle. From the diamond pyramid indentation marks in Fig. 2 we can see that the microhardness of M-A constituent is about four times higher than that of ferrite. Consequently, the M-A constituent should be easy to crack. In Fig. 3 we can see several cracked M-A constituents (as pointed by arrows) in front of the notch-root with crack plane almost perpendicular to the maximal principal stress. Figure 4 shows the fractograph in which a M-A constituent in front of the pre-crack initiates cleavage fracture.

From the above observation it can be assumed that in the present microstructure cleavage fracture may initiate at the sites of cracked M-A constituents, and only the large cracked M-A constituents that satisfy the Griffith condition of crack propagation,  $a_{cr} = 2\pi \gamma_p / \{\pi(1-\nu^2)\sigma_{cr}^2\}$ , can promote unstable cleavage fracture.

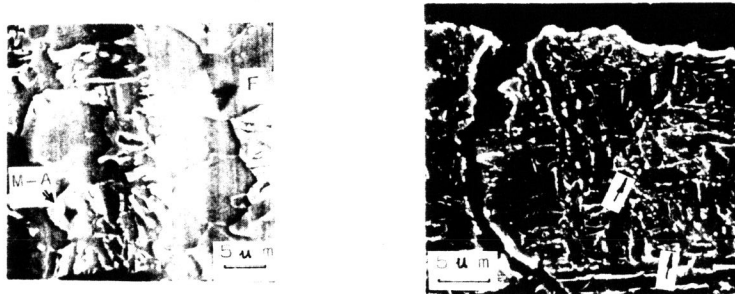


Fig. 2. The micro-hardness indentation marks on M-A constituent and ferrite, SEM. Fig. 3. The cracked M-A constituents in front of the notch.

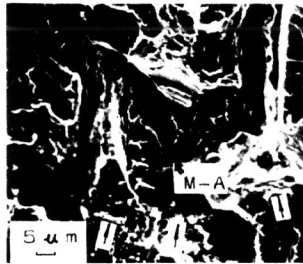


Fig. 4. Cleavage fracture initiated by a cracked M-A constituent. (Arrows point out the front of the pre-crack.)

STATISTICAL FRACTURE-MECHANICAL ANALYSIS OF CLEAVAGE FRACTURE

Quantitative metallographic analysis shows that the density of size distribution of M-A constituents can be approximated by the function  $f(d) = A \cdot d^{-b}$

where  $d$  is the thickness of M-A constituent. It is assumed that the probability density of the semi-length,  $a$ , of the cracks formed by M-A constituents is similar to the density of size distribution of M-A constituents that is  $f(a) = A \cdot a^{-b}$ , while  $f(a)$  satisfies

$$\int_{a_0}^{\infty} f(a) da = 1 \tag{1}$$

which leads to

$$A = (b-1) a_0^{b-1} \tag{2}$$

where  $a_0$  is the minimal semi-crack length,

$$f(a) = (b-1) a_0^{b-1} a^{-b} \tag{3}$$

and Suppose that the crack of length  $2a$ , formed by M-A constituent is a through-thickness crack. The probability of failure, for one crack under the applied stress,  $\sigma$ , is given by

$$F(\sigma) = \int_{a_{cr}}^{\infty} f(a) da = \left(\frac{\sigma}{\sigma_u}\right)^m \tag{4}$$

with

$$m = 2b-2 \tag{5}$$

and

$$\sigma_u = \left\{ \frac{2E\delta_p}{\pi(1-\nu^2)a_0} \right\}^{1/2} \tag{6}$$

which are the material parameters involved in the model, and  $\delta_p$  is the effective surface energy of ferrite. Using Equation (4) the fracture probability distribution function,  $P$ , of a specimen with  $N$  crack nuclei under the applied stress,  $\sigma$ , can be derived by means of the 'weakest link of a chain' concept as

$$P = 1 - \exp\{-NF(\sigma)\} = 1 - \exp\left\{-\frac{V}{V_u} \left(\frac{\sigma}{\sigma_u}\right)^m\right\} \tag{7}$$

where  $V_u = V/N$ , and  $V$  is the volume of the specimen, so  $V_u$  can be identified as the mean volume occupied by each crack nucleus, and is a constant for a given material.

From Equation (7) for smooth specimen with uniform stress within the whole plastically deformed volume  $V$  the statistical criterion of cleavage fracture is

$$\sigma^m \cdot V_s = \sigma_u^m V_u \ln \frac{1}{1-P} \tag{8}$$

For notched and cracked specimens, the stress field is non-uniform, but it can be considered that the maximum principal stress,  $\sigma_1$ , is constant within a volume element,  $dV$ . Hence, by means of the 'weakest link of a chain' concept, the fracture probability distribution function of a notched or cracked specimen can be derived as

$$P = 1 - \exp\left\{-\frac{\int \sigma_1^m dV}{\sigma_u^m V_u}\right\} \tag{9}$$

Thus, for the notched or cracked specimen the statistical criterion of cleavage fracture is

$$\int_{V_p} \sigma_1^m dV = \sigma_u^m V_u \ln \frac{1}{1-P} \tag{10}$$

Where  $V_p$  is also the volume of plastic zone, since the cleavage fracture nuclei can be initiated only after plastic deformation (Curry, 1980). For cracked specimen Equation (10) can be rewritten as

$$B_{cr} \sigma_y^m \left(\frac{K_{Ic}}{\sigma_y}\right)^4 \iint \left\{ \frac{\sigma_1(u, \theta)}{\sigma_y} \right\}^m \left\{ \frac{\bar{\sigma}_1(\theta)}{\sigma_1(0)} \right\}^m u du d\theta = \sigma_u^m V_u \ln \frac{1}{1-P} \tag{11}$$

where  $B_{cr}$  is the thickness of a cracked specimen,  $K_{Ic}$  is the fracture toughness,  $\sigma_1(u, \theta)/\sigma_y$  is given by FEM of McMeeking (1977) and Tracey (1976), and the angular factor  $\bar{\sigma}_1(\theta)/\sigma_1(0)$  of the maximum principal stress for cracked specimen is calculated by

$$\bar{\sigma}_1(\theta) = \frac{1}{2} \left\{ \bar{\sigma}_\theta(\theta) + \bar{\sigma}_r(\theta) \right\} + \left\{ \frac{1}{4} (\bar{\sigma}_\theta(\theta) - \bar{\sigma}_r(\theta))^2 + \bar{\sigma}_{r\theta}(\theta) \right\}^{1/2} \tag{12}$$

with  $\bar{\sigma}_\theta(\theta)$ ,  $\bar{\sigma}_r(\theta)$  and  $\bar{\sigma}_{r\theta}(\theta)$  computed by using the formula of Uhlmann and Co-workers (1976). The upper and lower limits of integration are 0 and 0.03 respectively for  $u$ , where the later is related to the position of the elastic-plastic interface directly ahead of the loaded crack, and  $-\pi$  and  $\pi$  for  $\theta$ .

Let 
$$F(m, n) \equiv \iint \left\{ \frac{\sigma_1(u, \theta)}{\sigma_y} \right\}^m \left\{ \frac{\bar{\sigma}_1(\theta)}{\sigma_1(0)} \right\}^m u du d\theta \tag{13}$$

which is a function of the Weibull modulus,  $m$ , and the power-law hardening exponent,  $n$ .

Based on Equation (11), the mean value of  $K_{Ic}$ , i.e.  $\bar{K}_{Ic} = \int_0^1 K_{Ic}(P) dp$ , can be derived and Equation (11) can be rewritten as

$$\sigma_u^m V_u = \left\{ \frac{\bar{K}_{Ic}}{\Gamma(1+\frac{1}{m}) \sigma_y} \right\}^4 \cdot B_{cr} \sigma_y^m \cdot F(m, n) \equiv C_{cr} \tag{14}$$

Similarly, from Equation (10) it follows that for notched specimen

$$\left(\sigma_f^*\right)^m \cdot \frac{B_n}{R^m} \cdot \rho^2 \cdot G(m, n) = \sigma_u^m V_u \ln \frac{1}{1-P} \tag{15}$$

and then,

$$\sigma_u^m V_u = \left\{ \frac{\bar{\sigma}_f \cdot n}{\Gamma(1+\frac{1}{m})} \right\}^m \cdot \left(\frac{B_n \rho^2}{R^m}\right) \cdot G(m, n) \equiv C_n \tag{16}$$

where  $\bar{\sigma}_{f,n}^*$  is the mean value of cleavage fracture stresses,  $\sigma_{f,n}^*$ , of several notched specimens,  $B_n$  and  $\rho$  are the thickness and notch-root radius of the specimen, respectively,  $R = \sigma_1^{max} / \sigma_y$  is the stress intensification of the notched specimen at fracture, and

$$G(m, n) = \int \int \left( \frac{\sigma_1(z, \theta)}{\sigma_y} \right)^m z dz d\theta \quad (17)$$

with  $Z = 1 + X$ , and  $X$  is the distance from the notch-root,  $\sigma_1(z, \theta) / \sigma_y$  is given by FEM of Griffiths and Owen (1971), which is a function of  $n$  and  $m$  too. From Equation (8) for the smooth specimen it can be derived that

$$\sigma_u^m V_u = \left\{ \frac{\bar{\sigma}_{f,s}^*}{\Gamma(1+\frac{1}{m})} \right\}^m \cdot V_s \equiv C_s \quad (18)$$

Because  $\sigma_u^m V_u$  is a constant for a given material, we should have  $C_{cr} = C_n = C_s$  from which the Weibull modulus,  $m$ , can be derived. For the simulated over-heated zone microstructure of welded 15MnVN steel used in this study, the computed result is

$$m = 11.5$$

and

$$\sigma_u^m V_u = 2.394 \times 10^{29} \text{ MPa}^{11.5} \text{ m}^3$$

CLEAVAGE FRACTURE STRESS,  $\sigma_f^*$ , AND THE EFFECTIVE VOLUME,  $V_e$

It is evident from Table 2 that the mean value of cleavage stresses for notched specimens is apparently higher than that of smooth specimens, and that for cracked specimens is the highest. This may be assumed to be due to the different effective volumes involved in the process of brittle fracture for different kinds of specimens. The effective volumes for them are defined and derived as follows. Equation (8), (11) and (15) can be rewritten as

$$(\sigma_{f,s}^*)^m \cdot V_{e,s} = \sigma_u^m V_u \text{Ln} \frac{1}{1-P} \quad (19)$$

$$(\sigma_{f,cr}^*)^m \cdot V_{e,cr} = \sigma_u^m V_u \text{Ln} \frac{1}{1-P} \quad (20)$$

$$(\sigma_{f,n}^*)^m \cdot V_{e,n} = \sigma_u^m V_u \text{Ln} \frac{1}{1-P} \quad (20)$$

where  $\sigma_{f,cr}^* = R \cdot \sigma_y$  by the definition of the cleavage fracture stress in the cracked specimen, and

$$V_{e,s} = V_s \quad (21)$$

$$V_{e,cr} = \frac{B_{cr}}{R^m} \cdot \left( \frac{K_{Ic}}{\sigma_y} \right)^4 \cdot F(m, n) \quad (23)$$

$$V_{e,n} = \frac{B_n}{R^m} \cdot \rho^2 \cdot G(m, n) \quad (24)$$

are the effective volumes of the three kinds of specimens, respectively. It should be pointed out that the stress intensification,  $R$ , for cracked specimens under plane strain, small-scale yielding condition is a fixed value, so, by definition, the cleavage stress  $\sigma_{f,cr}^* = R \cdot \sigma_y$  for several cracked specimens measured at a given temperature, i.e. with a given yield strength  $\sigma_y$ , should have the same value, and their mean value,  $\bar{\sigma}_{f,cr}^*$ , equals to  $\sigma_{f,cr}^*$ . In this case, only the effective volume,  $V_{e,cr}$  is a function of the probability distribution function,  $P$ . Its mean value  $\bar{V}_{e,cr} = \int_0^1 V_{e,cr}(P) dP$ .

For notched and smooth specimens, the cleavage stresses  $\sigma_{f,n}^*$  and  $\sigma_{f,s}^*$  are the function of  $P$ , and their mean values can be described as  $\bar{\sigma}_{f,n}^* = \int_0^1 \sigma_{f,n}^*(P) dP$  and  $\bar{\sigma}_{f,s}^* = \int_0^1 \sigma_{f,s}^*(P) dP$ , while the effective volumes,  $V_{e,n}$  and  $V_{e,s}$  are independent of  $P$ . Thus, Equations (19), (20) and (21) can be rewritten as

$$(\bar{\sigma}_{f,s}^*)^m \cdot \bar{V}_{e,s} = \sigma_u^m V_u \quad (25)$$

$$(\bar{\sigma}_{f,cr}^*)^m \cdot \bar{V}_{e,cr} = \sigma_u^m V_u \quad (26)$$

$$(\bar{\sigma}_{f,n}^*)^m \cdot \bar{V}_{e,n} = \sigma_u^m V_u \quad (27)$$

where the mean effective volumes are defined as

$$\bar{V}_{e,s} = \frac{V_s}{[\Gamma(1+\frac{1}{m})]^m} \quad (28)$$

$$\bar{V}_{e,cr} = \frac{B_{cr}}{R^m} \left\{ \frac{K_{Ic}}{\Gamma(1+\frac{1}{m}) \sigma_y} \right\}^4 \cdot F(m, n) \quad (29)$$

$$\bar{V}_{e,n} = \frac{B_n \rho^2}{[\Gamma(1+\frac{1}{m}) \cdot R]^m} \cdot G(m, n) \quad (30)$$

The values of  $\bar{\sigma}_f^*$  and  $\bar{V}_e$  calculated from Equations (28), (29) and (30) are listed in Table 2. It is obvious that the larger  $\bar{V}_e$  is, the lower  $\bar{\sigma}_f^*$  will be.

It is worth noting that from Equation (23) and Table 2 the effective volume,  $V_{e,cr}$ , of a cracked specimen is much less than its plastically deformed volume,  $V_p$ , since  $V_{e,cr}$  represents essentially the volume of the zone near the location of maximum stress ahead of the precrack. So does the effective volume for a notched specimen. From Fig. 3 it can be seen that the origin which initiates the cleavage fracture lies at the zone of highest stress in front of the crack-tip. The less  $V_e$  is, the lower the probability of finding a large activated crack nucleus formed by a M-A constituent will be, so that the applied stress needed for propagating the crack nucleus is higher, and vice versa.

For a given material  $m, \sigma_u$  and  $V_u$  are constants, we can use the following Equation (31) to represent Equations (25), (26) and (27).

$$\text{Ln} \bar{V}_e = \text{Ln} (\sigma_u^m V_u) - m \text{Ln} \bar{\sigma}_f^* \quad (31)$$

Thus, points  $(\text{Ln} \bar{\sigma}_f^*, \text{Ln} \bar{V}_e)$  for smooth, notched and cracked specimens should lie on a straight line with a slope of  $m$ , and  $m=11.5$  for the present material. This is consistent with the result of the experiment shown in Fig. 5, and the four pairs of  $\bar{\sigma}_f^*$  and  $\bar{V}_e$  listed in Table 2 can be regressed as  $\text{Ln} \bar{V}_e = 88.405 - 11.503 \text{Ln} \bar{\sigma}_f^*$  with the regression coefficient  $r = 0.99997$ . Further, there is a definite relationship between  $\bar{\sigma}_f^*$  measured from the specimens of the three kinds, which can be expressed as

$$\bar{\sigma}_{f,cr}^* = \left( \frac{\bar{V}_{e,n}}{\bar{V}_{e,cr}} \right)^{1/m} \cdot \bar{\sigma}_{f,n}^*$$

and

$$\bar{\sigma}_{f,s}^* = \left( \frac{\bar{V}_{e,n}}{\bar{V}_{e,s}} \right)^{1/m} \cdot \bar{\sigma}_{f,n}^*$$

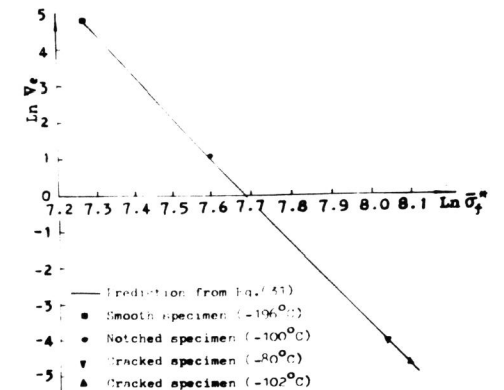


Fig. 5. The relationship between  $\bar{\sigma}_f^*$  and  $\bar{V}_e$

## CONCLUSION

1. The cleavage stresses measured by smooth, notched and cracked specimens are very different if they are defined by the maximum principal stress at fracture.
2. M-A constituent in simulated over-heated zone of welded 15MnVN steel serves as the crack nucleus of cleavage fracture.
3. Weibull type statistical formulae for cleavage fracture are derived based on the 'weakest link theory' and the measured size distribution of crack nuclei formed by cracking M-A constituents.
4. By making use of the above statistical cleavage fracture criterion the mean effective volumes,  $\bar{V}_e$ , involved in fracture process for smooth, notched and cracked specimens are defined and the volume effect on cleavage stress can be expressed by a simple explicit relation as

$$(\bar{\sigma}_f^*)^m \cdot \bar{V}_e = \sigma_u^m V_u$$

The experimental results for simulated HAZ structure of welded 15MnVN steel are consistent with the prediction. The mean effective volume  $\bar{V}_e$  for notched and cracked specimens can be interpreted as the volume of the zone near the location of maximum stress which can be involved in cleavage fracture process.

## ACKNOWLEDGEMENTS

The help of Mr. Li You-dao, Mr. Cheng Mo-yi and Ms. Wei Shu-xiang in testing and computing is gratefully acknowledged.

## REFERENCES

- Beremin, F.M. (1981) In D. Francois (Ed.) Advances in Fracture Research, Vol. 2, Pergamon Press, Paris. PP. 825-832
- Curry, D.A. and J.F. Knott (1976). Metal Science, 10, 1-6.
- Curry, D.A. (1980). Metal Science, 14, 319-326.
- Griffiths, J.R. and D.R.J. Owen (1971). J. Mech. Phys. Solids, 19, 419-431.
- Knott, J.F. (1966). J. Iron Steel Inst., 204, 104-111.
- McMeeking, R.M. (1977). J. Mech. Phys. Solids, 25, 357-381.
- Ritchie, R.O., J.F. Knott and J.R. Rice (1973). J. Mech. Phys. Solids, 21, 395-410
- Tracey, D.M. (1976). ASME Series H. J. Eng. Mat. Tech. 98, 146-151.
- Uhlmann, W., Z. Knesl, M. Kuna and Z. Bilek (1976). Int. J. Fract., 12, 507-509.